Molecular Therapy
Oncolytics
Original Article

AMERICAN SOCIETY of GENE & CELL THERAPY

High-Affinity DARPin Allows Targeting of MeV to Glioblastoma Multiforme in Combination with Protease Targeting without Loss of Potency

Jan R.H. Hanauer,[1,2] Vivian Koch,[1] Ulrich M. Lauer,[3] and Michael D. Mühlebach[1,2]

[1]Oncolytic Measles Viruses and Vaccine Vectors, Paul-Ehrlich-Institut, 63225 Langen, Germany; [2]Veterinary Medicine, Paul-Ehrlich-Institut, 63225 Langen, Germany; [3]Department of Medical Oncology and Pneumology, University Hospital, University of Tübingen, 72076 Tübingen, Germany

Measles virus (MeV) is naturally cytolytic by extensive cell-to-cell fusion. Vaccine-derived MeV is toxic for cancer cells and is clinically tested as oncolytic virus. To combine the potential of MeV with enhanced safety, different targeting strategies have been described. We generated a receptor-targeted MeV by using receptor-blind viral attachment protein genetically fused to designed ankyrin repeat protein (DARPin) binding domains specific for the epidermal growth factor receptor (EGFR). To reduce on-target toxicity for EGFR$^+$ healthy cells, we used an engineered viral fusion protein activatable by tumor-associated matrix metalloproteases (MMPs) for additional protease targeting. The dual-targeted virus replicated exclusively on EGFR$^+$/MMP$^+$ tumor cells but was safe on healthy EGFR$^+$ target cells, primary human keratinocytes. Nevertheless, glioblastoma and other tumor cells were efficiently killed by all targeted viruses, although replication and oncolysis were slower for protease-targeted MeV. *In vivo*, efficacy of EGFR-targeted MeV was virtually unimpaired, whereas also dual-targeted MeV showed significant intra-tumoral spread and efficacy and could be armed with a prodrug convertase. The use of DARPin-domains resulted in potent EGFR-targeted MeV and for the first time effective dual retargeting of an oncolytic virus, further enhancing tumor selectivity. Together with powerful cell-toxic genes, the application as highly tumor-specific platform is promising.

INTRODUCTION

Measles virus (MeV) is a member of the *paramyxoviridae* and the causative agent of the measles. Replicating attenuated vaccine strains of MeV are available that have revealed an excellent safety profile while being administered as measles vaccine in millions of doses. MeV encodes two surface glycoproteins: the hemagglutinin (H) and the fusion protein (F). H is responsible for viral attachment by binding of the viral receptors: signaling lymphocyte activation molecule (SLAM)[1] on activated lymphocytes and myeloid cells and nectin 4[2,3] on epithelial cells. MeV vaccine strains additionally use ubiquitously expressed CD46[4,5] for cell entry. Upon binding, H activates F, which then initiates membrane fusion. However, F is only active if previously cleaved by an activating protease, furin, usually during F's transport through the trans-Golgi network. The CD46 tropism of MeV vaccines results in an inherent preference for tumors, since CD46, the major complement regulatory protein, is often upregulated on tumor cells to evade complement lysis.[6] Consequently, a MeV Edmonston B vaccine strain-derived molecular clone is currently tested as an oncolytic virus in clinical trials to treat ovarian carcinoma, glioblastoma multiforme, multiple myeloma, or mesothelioma[7] and revealed good tolerability and first indications of efficacy.[8] However, as CD46 is expressed on all human nucleated cells, MeV's inherent tumor-specificity is relative. To gain a higher specificity, the natural receptor tropism of H was ablated[9] and substituted by C-terminal fusion of a selected binding domain attaching to the tumor antigen of choice as a target receptor.[10] Resulting recombinant MeVs have a fully retargeted entry tropism solely determined by the targeting domain, usually a single chain antibody fragment (scFv)[11] or alternatively designed ankyrin repeat proteins (DARPins).[12,13] Examples of such fully retargeted MeV are viruses retargeted to EGFR or the rearranged variant, EGFRvIII,[14,15] especially expressed in glioblastoma.

Gliomas are the most frequent primary (30%) and secondary (80%) brain tumors in adults.[16] 54% of all gliomas are classified as glioblastoma multiforme, which is characterized by its invasive growth, which is assisted by the upregulation of tumor-associated proteinases and results in extraordinary malignancy. Standard therapy results in a median overall survival of merely 15 to 17 months.[17,18] Thus, there is a tremendous requirement for new effective treatment strategies. EGFR or the highly tumor-specific deletion variant, EGFRvIII, where exons 2–7 in the extracellular domain of EGFR are deleted, are oncogenic driver tumor antigens overexpressed by GBM in 30%–50% of patients,[19,20] but also in other epithelial derived tumors. Therefore, EGFR has been the point of attack of different targeted therapies such as monoclonal antibodies or small molecule inhibitors. These have become standards of care for certain tumor entities such as colorectal carcinoma.[21] Targeting MeV to glioblastoma via scFvs and DARPins is effective.[12,14,15] Because MeV retargeted by DARPins

Received 16 September 2019; accepted 14 October 2019;
https://doi.org/10.1016/j.omto.2019.10.004.

Correspondence: Michael D. Mühlebach, Veterinary Medicine, Paul-Ehrlich-Institut, 63225 Langen, Germany.
E-mail: michael.muehlebach@pei.de

Table 1. Overview of Studied Viruses

Virus	DARPin	K_D (nmol/L)	Protease Activation	Transgene
MV_{NSe}	–	–[a]	–[b]	GFP
MV-E.01	E.01	0.50	–[b]	GFP
MV-E.68	E.68	0.70	–[b]	GFP
MV-E.69	E.69	15.00	–[b]	GFP
MV-MMPA1	–	–[a]	MMP	GFP
MV-MMPA1-E.01	E.01	0.50	MMP	GFP
MV-MMPA1-E.01-SCD	E.01	0.50	MMP	SCD

Abbreviations: DARPin, designed ankyrin repeat protein; KD, dissociation constants of DARPin as measured by equilibrium titration.
[a]Non-targeted MeV using CD46 for entry into cells.
[b]Unmodified MeV F protein is activated by ubiquitous furin-like proteases in the trans-Golgi network during surface transport.

can reveal higher targeted toxicity and efficacy than scFv-targeted viruses,[12] we focused now on the therapeutic efficacy of EGFR-targeted DARPin-MeV for the treatment of GBM. For this purpose, we had used DARPins E.01, E.68, and E.69[22] to generate EGFR-targeted MeV.[12]

One concern of therapies targeting EGFR is the expression of this receptor as a non-exclusive tumor antigen in healthy epithelial tissues. The use of monoclonal anti-EGFR antibodies or EGFR inhibitors revealed significant side-effects on healthy EGFR-positive tissue.[23,24] These side effects can cause a significant decrease in the quality of life, often narrow the therapeutic window, and may even require cessation of the targeted therapy.[25] In principle, similar issues can be expected for all potent therapeutics targeted to EGFR. Thus, especially for targeted MeV, a second layer of targeting, which limits the local spread of virus to tumor tissue, should be helpful to reduce side-effects due to on-target infection of healthy cells. Such a second layer of targeting is available by protease targeting, i.e., targeting the indispensable proteolytic maturation of the F protein to tumor-associated matrix metalloproteinases (MMPs).[26] Such MMP activatable MeVs can only replicate in MMP-positive tumor tissue[27] but have revealed conserved cytolytic activity.[26] Glioblastomas with their highly invasive phenotype also express MMPs for this purpose.[28] Therefore, dual-targeted MeV being selective for invasive, EGFR-expressing tumors should be excellently suited for treatment of GBM.

In this study, we therefore aimed to first analyze the oncolytic efficacy of solely EGFR-targeted DARPin-MeV with different affinities for the target-receptor, or protease-targeted MV-MMPA1 against a collection of different tumor cell lines, especially derived from glioblastoma. Next, we aimed to generate a dual-targeted MeV based on MV-E.01, the most efficient virus with highest EGFR-affinity, and on protease-targeted MV-MMPA1. The resulting dual-targeted virus MV-MMPA1-E.01 is dependent on both EGFR-expression and invasive growth of tumor cells. Thus, it minimizes undesired on-target infection of primary human keratinocytes while still showing anti-tumoral effectiveness *in vitro* and *in vivo* in two different GBM xenograft models. Finally, we characterized an armed dual-targeted virus on one of these xenograft models for synergies of widespread tumor infection and conversion of a prodrug *in situ* by the additionally encoded super-cytosine deaminase prodrug convertase.

RESULTS

Cytolytic Activity of EGFR-Targeted DARPin-MeV

To further characterize recombinant oncolytic MeVs, which are retargeted with the help of different DARPins binding to EGFR (Table 1),[12] the analysis of their respective cytolytic efficacy was expanded to further cell lines and the kinetics of killing. In this context, we put a special focus on a tumor entity well known for the critical role of EGFR-overexpression, i.e., glioblastoma multiforme (GBM). Three glioblastoma cell lines (LNT-229, LNZ-308, and U87mg), a fibrosarcoma cell line (HT1080), a hepatocellular carcinoma cell line (Huh7), and an ovarian adenocarcinoma cell line (SK-OV-3), which all had been demonstrated to have high densities of EGFR at their surface,[12] were used for analysis. All tumor cell lines were infected by MeV, i.e., MV-E.01, MV-E.68, or MV-E.69, which are targeted to EGFR-positive cells with the help of three different EGFR-specific DARPins (E.01, E.68, or E.69, respectively) fused to their hemagglutinins, or the parental, non-targeted virus MV_{NSe}. Subsequently, the residual metabolic activity of infected cells was compared to mock infected controls over a period of 1 week post infection (p.i.) to monitor cell killing by the different viruses (Figure 1A).

In general, the metabolic activity was reduced in all infected cell lines using any virus already starting at 24 h p.i., indicating early cell killing. For infected cultures of U87mg or Huh7 cells, no residual metabolic activity was found after 168 h or 48 h p.i., respectively, indicating complete eradication of tumor cells by infection with any virus by these time points. For LNZ-308 cells, a complete eradication was achieved by all but one virus, i.e., MV-E.69, by 72 h p.i. In contrast, infection of SK-OV-3 cells resulted in at least 10% residual metabolic activity at the latest analyzed time point of 168 h p.i., while infected HT1080 cultures displayed a mixed phenotype after infection with the different viruses, with very low residual metabolism after infection with MV_{NSe} or MV-E.01, but high metabolism after infection with MV-E.69. In infected LNT-229 cultures, viability even started to increase after minimal activity was reached in the time span of 48 h to 72 h p.i.

Overall, the oncolytic efficacy of DARPin-MeV retargeted by DARPin E.01 with the highest affinity for EGFR (0.5 nM) was almost identical to the efficacy of non-targeted MV_{NSe}. On LNT-229 cells, the cytotoxicity of the EGFR-targeted viruses MV-E.01 and MV-E.68 seems to be even higher than non-targeted MV_{NSe}. After infection by targeted MeV, the metabolic activity of infected LNT-229 cells reached a minimum activity 48 h p.i. while it took 72 h p.i. using non-targeted MV_{NSe}. In general, MeV retargeted by DARPin-E69 with lower affinity to EGFR (15 nM) had in general a less cytotoxic phenotype.

These metabolic data were supported by colony-forming assay. For that purpose, all tumor cell lines were infected with the different

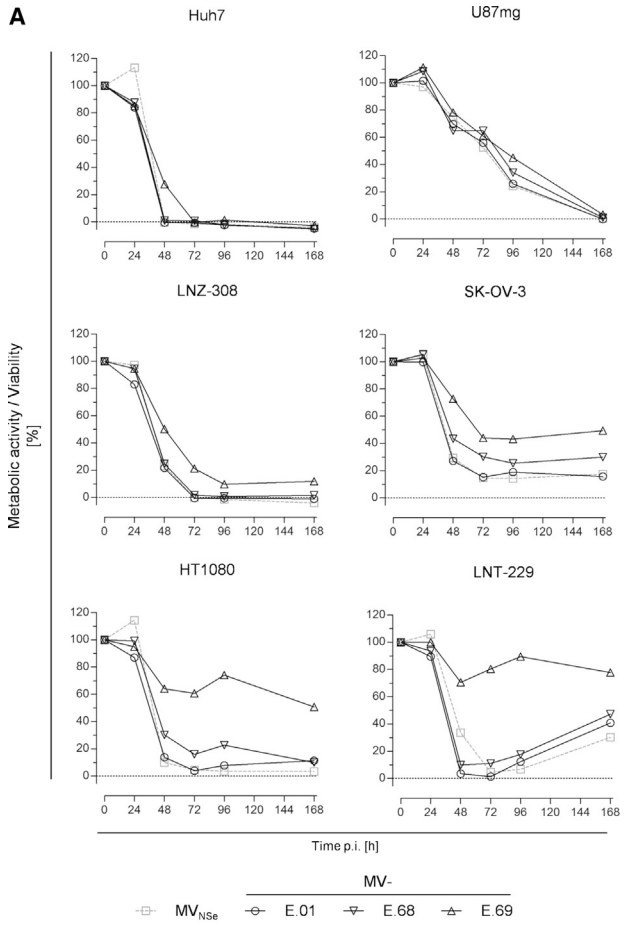

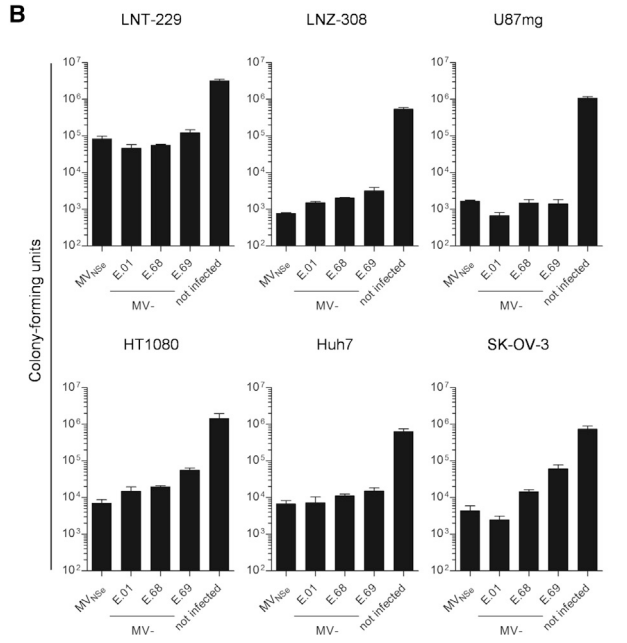

Figure 1. Cytolytic Efficacy of EGFR-Targeted MeV *in vitro*

(A) The human glioblastoma cell lines U87mg (upper left), LNZ-308 (middle right), LNT-229 (lower left), the hepatocellular carcinoma cell line Huh7 (upper right), the ovarian carcinoma cell line SK-OV-3 (middle left), or the fibrosarcoma cell line HT1080 (lower right) were infected with parental MV_{NSe} or EGFR-targeted DARPin-MeVs, i.e., MV-E.01, MV-E.68, or MV-E.69 as indicated below the graphs (MOI = 1) and viability was determined at indicated time points by MTT assay. Depicted is metabolic activity indicating viability relative to the mock infected control culture. One representative out of 3 independent experiments each consisting of 4 replicates. (B) Indicated cell lines were infected in triplicates (MOI = 0.1) with non-targeted MV_{NSe}, indicated viruses MV-E.01, MV-E.68, or MV-E.69 targeted against EGFR, or left untreated, and colony-forming capacity of infected cultures was assessed 72 h p.i. Colony numbers were counted after further 2–3 weeks. Error bars, SD.

targeted and non-targeted viruses (MOI = 0.1) and survival of colony-forming entities was quantified (Figure 1B). The colony-forming assay resulted in a very similar pattern as the MTT assay measuring metabolic activity: all analyzed viruses displayed a cytotoxic phenotype and were found to reduce the number of colony-forming units (CFUs) compared to mock infected cultures by at least 75%. MV-E.01 and the parental virus showed a similar cytotoxicity causing a reduction in CFU of 97%–99.8%. Interestingly, the cytotoxicity of MV-E.01 was even slightly higher on some tumor cell lines (LNT-229, U87mg, and SK-OV-3), whereas it was reduced on the others. MV-E.68 and MV-E.69 were in general less cytotoxic in the colony-forming assay. The maximal effect of these viruses was observed on the Huh-7 cells but significantly reduced in others compared to MV_{NSe} or MV-E.01. Thus, all tested tumor cell lines could be readily infected and killed by high-affinity EGFR-targeted MeV. Especially the three GBM cell lines were found to be quite susceptible to infection and killing by EGFR-targeted DARPin-MeV, as expected. Thus, GBM got even more in our focus for the next analyses.

Targeting of EGFRvIII-Positive Tumor Cells

Because glioblastoma cells often express a truncated version of EGFR, the EGFR-variant III (EGFRvIII), we next analyzed entry receptor function of this variant for EGFR-targeted DARPin-MeVs. This EGFR mutant bears an extensive deletion in the extracellular domains. Thus, conservation of αEGFR-DARPins' binding surfaces on EGFRvIII remained to be elucidated. To address this question, Chinese hamster ovary (CHO) cells stably expressing EGFR or EGFRvIII (but not any other primate-specific receptors for MeV) were used. Both cell lines (CHO-EGFR, CHO-EGFRvIII) were infected by the GFP-enocding EGFR-targeted DARPin-MeVs (MOI = 0.3), and infection and spread of the viruses was documented by GFP expression and syncytia formation (Figure 2). CHO-EGFR cells were infected by all EGFR-targeted DARPin-MeV, as demonstrated before.[12] In contrast, MV-E.01 and MV-E.68, but not MV-E.69 infected CHO-EGFRvIII cells (the latter finding being referred especially to the lower affinity to EGFR (15 nM) of DARPin-E69 used to retarget MeV). Thus, DARPin-MeV retargeted by DARPins E.01 or E.68 were demonstrated to be able to make functional use of EGFRvIII for cell entry and spread. Therefore, these variants are suited for cancer cells expressing EGFR or EGFRvIII, as desired for glioma therapy.

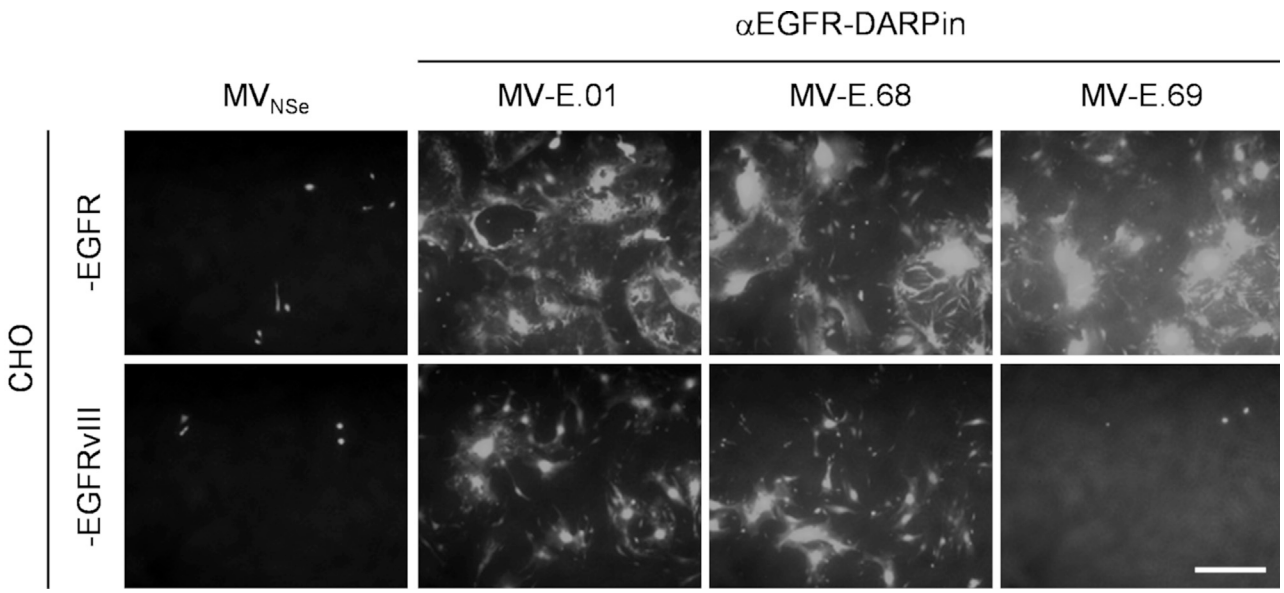

Figure 2. Receptor Tropism of EGFR-Targeted MeV

Receptor-transgenic CHO cell lines expressing either human wtEGFR or the truncated variant III (as indicated) were infected with different EGFR-targeted DARPin-MeV (MOI = 0.3). Infected cultures were analyzed 48 h after infection by fluorescence microscopy. Representative pictures are shown. Scale bar, 400 μm.

Increasing Tumor Specificity Utilizing MMP Activation

EGFR-targeted therapies bear in principle the risk of side effects due to EGFR expression also on healthy epithelial tissue. Therefore, we next aimed to use the excellent efficacy profile of MV-E.01 to combine receptor targeting and protease targeting to be able to suppress potential off target-effects of EGFR-targeted MeV on non-tumorous cells. For that purpose, a dual-targeted recombinant virus MV-MMPA1-E.01 was generated (Table 1). This virus should require both target receptor expression and MMP activation, as found in highly invasive GBM.[28] To first prove the principle suitability of protease-targeted MV-MMPA1 (Table 1) also for GBM, we infected two different GBM cell lines, namely LNZ-308 and U87mg, as well as the protease targeting-permissive (EGFR-positive) HT1080 fibrosarcoma cells with MV-MMPA1 in direct comparison to non-targeted MV$_{NSe}$ (Figure 3). Indeed, all three tested cell lines allowed spread of protease-targeted MV-MMPA1. Especially on LNZ-308 cells, patterns of infection were barely distinguishable between targeted and non-targeted MeV. Thus, protease targeting can be also used for development of therapeutic MeV against GBM and for combination with EGFR-targeting to render dual-targeted viruses.

In a next step, the genome encoding MV-MMPA1-E.01 (Table 1) was cloned by replacing the transcription unit of the native fusion protein by a gene cassette encoding MMP-activatable F-MMPA1[26,27] (Figure 4A). 293T-F cells stably expressing MeV-F protein were generated and used for better rescue efficacy of protease-targeted viruses by providing active F in rescue cells, *in trans*. Dual-targeted MV-MMPA1-E.01 viruses were rescued in 293T-F cells in co-culture with EGFR- and MMP-positive HT1080 cells. The recombinant virus was amplified on HT1080 cells and grew to maximal titers in the range of 1×10^6 to 1×10^7 tissue culture infective dose ($TCID_{50}$)/mL.

Next, MV-MMPA1-E.01 was analyzed for identity and specificity. Viral RNA was isolated and reversely transcribed and the transcription units encoding both modified glycoproteins were sequenced demonstrating integrity of the virus' genome (data not shown). To demonstrate expression of the modified glycoproteins by the respective recombinant MeV, we infected HT1080 cells with MV-MMPA1-E.01, MV-MMPA1, MV-E.01, or parental MV$_{NSe}$ and lysates of infected cells were checked for expression of MeV-F or MeV-H by immunoblot analysis (Figure 4B). EGFR-targeted MV-E.01 and dual-targeted MV-MMPA1-E.01 both expressed an H protein with an apparent size of approximately 100 kDa that is about 20 kDa larger than native MeV-H (as expected for targeted H-DARPin proteins). MMP-targeted MV-MMPA1 and MV-MMPA1-E.01 both express an F protein with an inverted ratio of unprocessed F_0 to activated F_1 compared to native F as expressed by MV$_{NSe}$ and MV-E.01. This indicates the reduced procession of MMP-activatable F variants. Thus, MV-MMPA1-E.01 encodes both targeted glycoproteins and facilitates their expression in infected cells.

Moreover, targeting of MV-MMPA1-E.01 to just EGFR- and MMP-double positive cells was demonstrated on HT1080 cells using a broad spectrum MMP inhibitor. For this purpose, HT1080 cells were infected with parental non-targeted MV$_{NSe}$, EGFR-targeted MV-E.01, MMP-targeted MV-MMPA1, or dual-targeted MV-MMPA1-E.01 in the absence (Figure 4C, upper row: −) or presence (Figure 4C, lower row: +) of MMP inhibitor GM6001. Infection and virus spread by cell-cell fusion was documented at 48 h p.i. (Figure 4C).

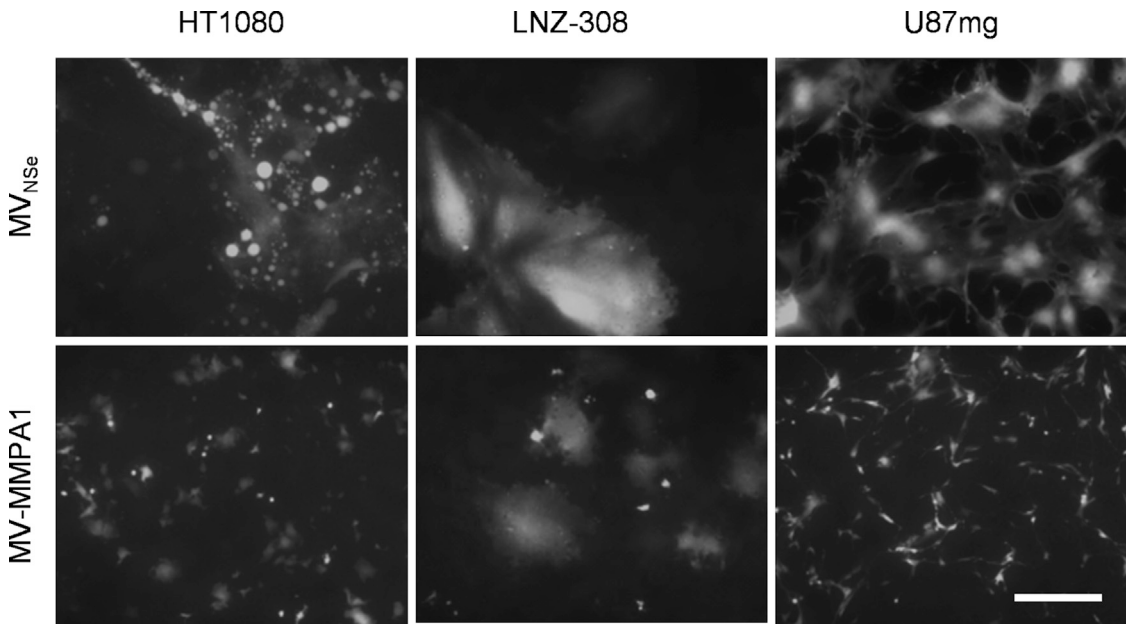

Figure 3. Susceptibility of GBM Cell Lines for Protease-Targeted MeV

LNZ-308 and U87mg glioblastoma cell lines were infected in parallel to HT1080 fibrosarcoma cells with protease-targeted MV-MMPA1, or parental, non-targeted MV$_{NSe}$ (MOI = 0.3). Infected cultures were analyzed 48 h after infection by fluorescence microscopy. Representative pictures are shown. Scale bar, 400 μm.

Parental MV$_{NSe}$ and MV-E.01 infected the cells and readily spread as multi-nucleated syncytia formed, regardless of the inhibitor. In contrast, pre-activated MV-MMPA1 and MV-MMPA1-E.01, which had been pre-activated by the MMP-positive producer cells, initially infected all HT1080 cultures, but formation of syncytia, i.e., cell-to-cell spread, was only observed in untreated HT1080 cells (Figure 4C, two upper panels to the right). Blockade of MMP activity resulted in inhibition of virus spread. Notably, syncytia formation caused by MMP-activatable viruses MV-MMPA1 or MV-MMPA1-E.01 is reduced in comparison to MV$_{NSe}$ or MV-E.01 expressing native MeV-F.

Protection of Primary Human Keratinocytes against Infection by Dual-Targeting

Because keratinocytes are positive for EGFR, significant adverse effects of anti-EGFR mAb therapies are related to off-target effects on this cell type. Moreover, keratinocytes represent target cells for wild-type MeV infections[29] and, because susceptibility is due to nectin-4 expression, should be susceptible for all MeV strains, in principle.[12] Thus, off-target effects for oncolytic therapy using solely EGFR-targeted MeV could be expected on-target for this cell population, but should be abolished using MMP- or dual-targeted viruses. To characterize the safety profile of our (EGFR-targeted) MeV *in vitro*, we therefore analyzed infection of primary human keratinocytes by those viruses (Figure 4D). While non-targeted MV$_{NSe}$ and EGFR-targeted MV-E.01 readily infected keratinocytes of 3 different healthy human donors and induced extensive cell-to-cell fusion, both MMP-targeted MV-MMPA1 and dual-targeted MV-MMPA1-E.01 initially infected some keratinocytes, but infection did not spread and no cell-to-cell fusion became evident. Thus, the enhanced safety of dual-targeted MeV was thereby shown on a highly relevant primary target cell of EGFR-targeted therapies.

Cytolytic Efficacy of Dual-Targeted Virus

To further characterize the impact of combined dual EGFR- and MMP-targeting on the oncolytic efficacy of the respective MeV, we determined kinetics of viral cytotoxicity by analysis of metabolic activity of infected target cells combined with analyzing the viral replication. For this purpose, we used the fibrosarcoma cell line HT1080 and two GBM cell lines, LNZ-308 and U87mg. These cells were infected with MV$_{NSe}$, MV-E.01, MV-MMPA1, or MV-MMPA1-E.01, and analyzed for cytotoxic effects and spread of the virus (Figure 5A, upper panel). All cells lost metabolic activity after they were infected with the different MeVs. While both GBM lines revealed a steady decline of viability of infected cultures, viability of HT1080 cells rebounded at 168 h p.i. for non-targeted MV$_{NSe}$ and just EGFR-targeted MV-E.01 after minimal viability at 96 h p.i. In general, cell killing by MMP-activatable viruses (MV-MMPA1 and MV-MMPA1-E.01) appears to be delayed and did not reach the same minimal viability at the end of our experiment. Nevertheless, the phenotype of MMP-targeted viruses appears as a constant, but slower decline of viability of infected cultures. In any case, targeting of EGFR using DARPin E.01 with the highest receptor affinity did not attenuate the phenotype of non-targeted or protease-targeted MeV on any of the tested cell lines.

In parallel, the cell lines were infected with the same four MeVs (MOI of 0.03) and viral growth was determined by monitoring

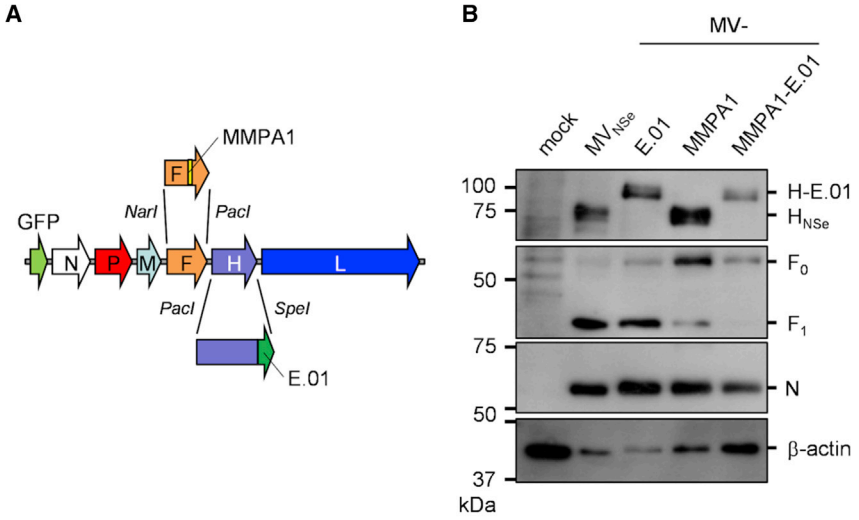

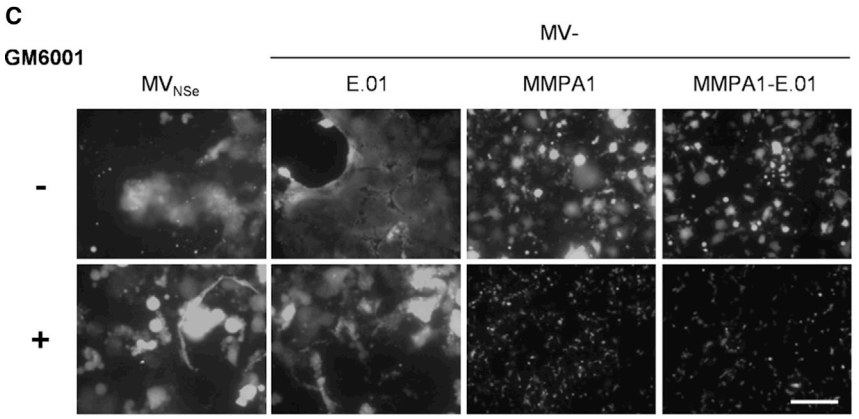

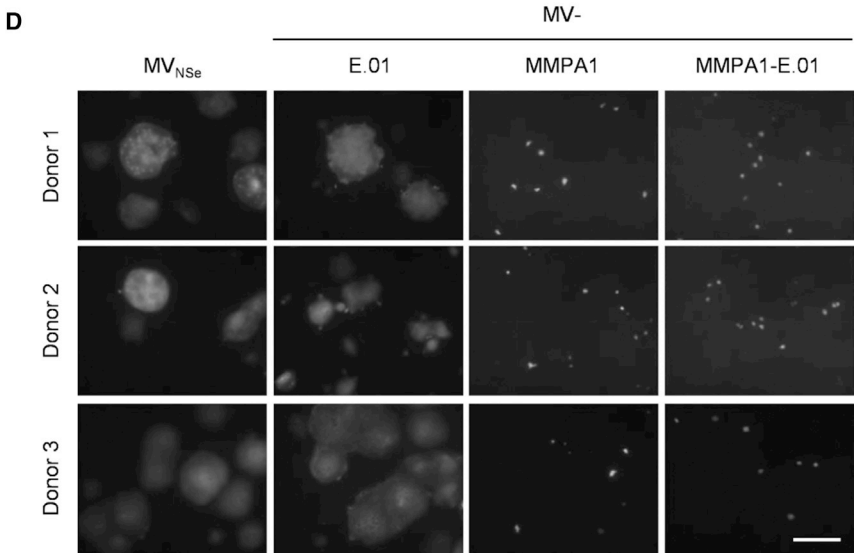

Figure 4. Generation and Tropism of Dual-Targeted Viruses

(A) Schematic representation of dual-targeted MeV genome with cloning sites used for exchange of the H and F gene cassette. (B) Immunoblot for detection of EGFR- (MV-E.01), protease- (MV-MMPA1), or dual-targeted (MV-MMPA1-E.01) and parental (MV_{NSe}) viruses' proteins. Lysates of infected HT1080 cells 48 h after infection (MOI = 0.1) were analyzed for indicated proteins. Protein content was normalized to MeV-N and β-actin. (C and D) EGFR- and MMP-positive HT1080 fibrosarcoma cells (C) or primary human keratinocytes (D) were infected with EGFR- (MV-E.01), protease- (MV-MMPA1), or dual-targeted (MV-MMPA1-E.01) MeV in direct comparison to parental, non-targeted MV_{NSe} (MOI = 0.3). HT1080 cells were infected in the absence or presence of the broad-spectrum MMP inhibitor GM6001 (indicated by ± MMP activity). Infected cultures were analyzed at 48 h after infection by fluorescence microscopy. Representative pictures are shown. Scale bar, 400 μm.

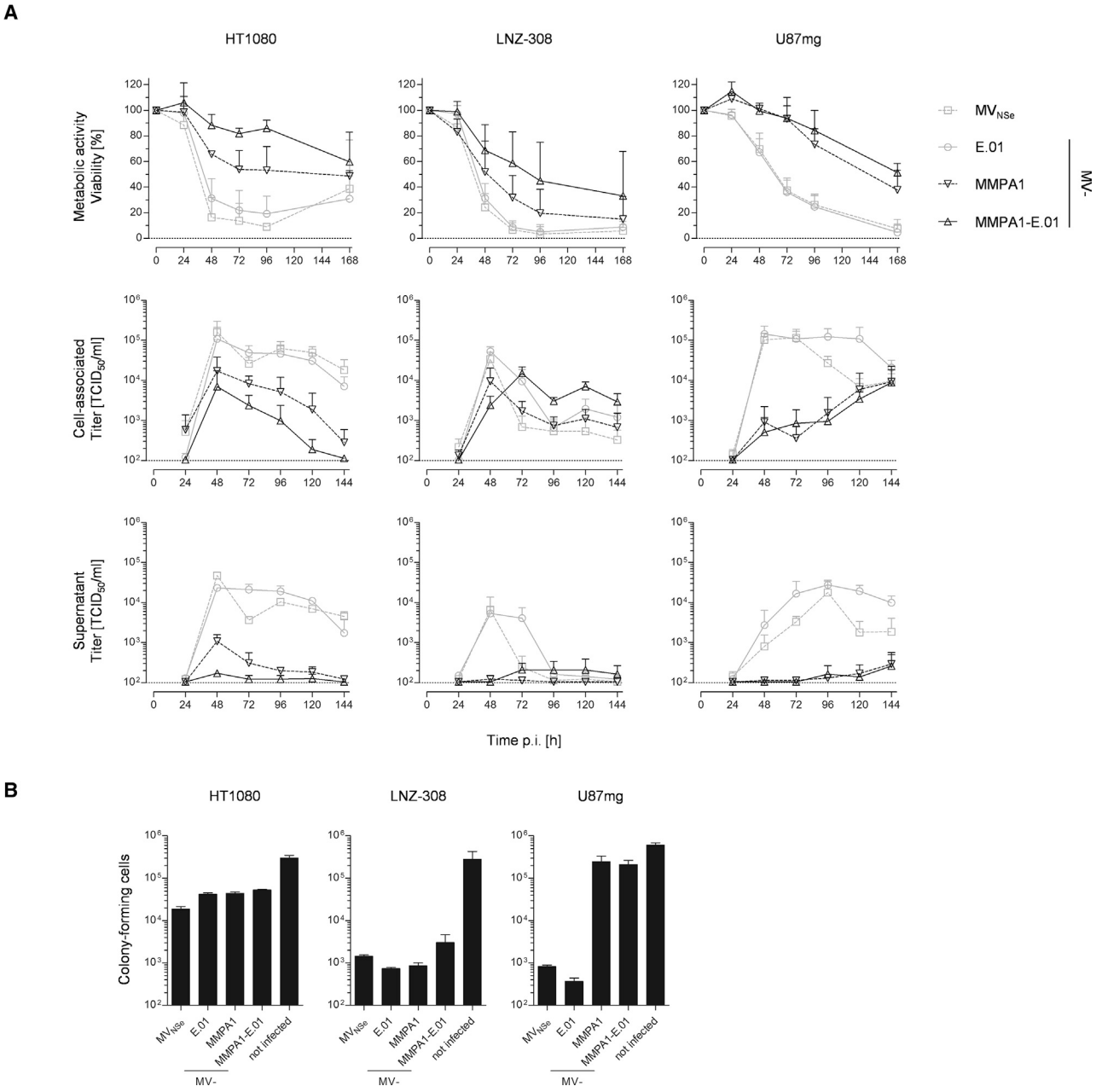

Figure 5. Cytolytic Efficacy of Dual-Targeted MeV *in vitro*

(A) The human fibrosarcoma cell line HT1080 (left column) or the human glioblastoma cell lines LNZ-308 (middle column) or U87mg (right column) were infected with parental MV_{NSe}, EGFR-targeted MV-E.01, protease-targeted MV-MMPA1, or dual-targeted MV-MMPA1-E.01 (MOI = 1) and viability was determined at indicated time points by MTT assay (upper row); mean of 4 independent experiments each consisting of 4 replicates. Moreover, the multi-step growth analysis of recombinant MeV on these cells after infection at an MOI of 0.03 is shown, depicting cell-associated (middle row) or released viruses (lower row) titered on HT1080 cells. Mean of 3 independent experiments, error bars indicate SD. (B) Indicated cell lines were infected (MOI = 0.1) with non-targeted MV_{NSe}, indicated EGFR-, protease-, or dual-targeted viruses, or left untreated, and colony forming capacity of infected cultures was assessed 72 h p.i. Colony numbers were counted after further 2–3 weeks. Error bars, SD; 1 representative out of 3 independent experiments.

cell-associated and supernatant titers (Figure 5A, middle and lower panels). All viruses productively replicated on the analyzed cell lines. Thereby, cell-associated titers were by one order of magnitude higher than titers of extracellular released virus, as expected for MeV, in general. Maximal titers of parental viruses with no MMP-targeting were reached between 48 to 72 hpi, whereas growth of the MMP-targeted

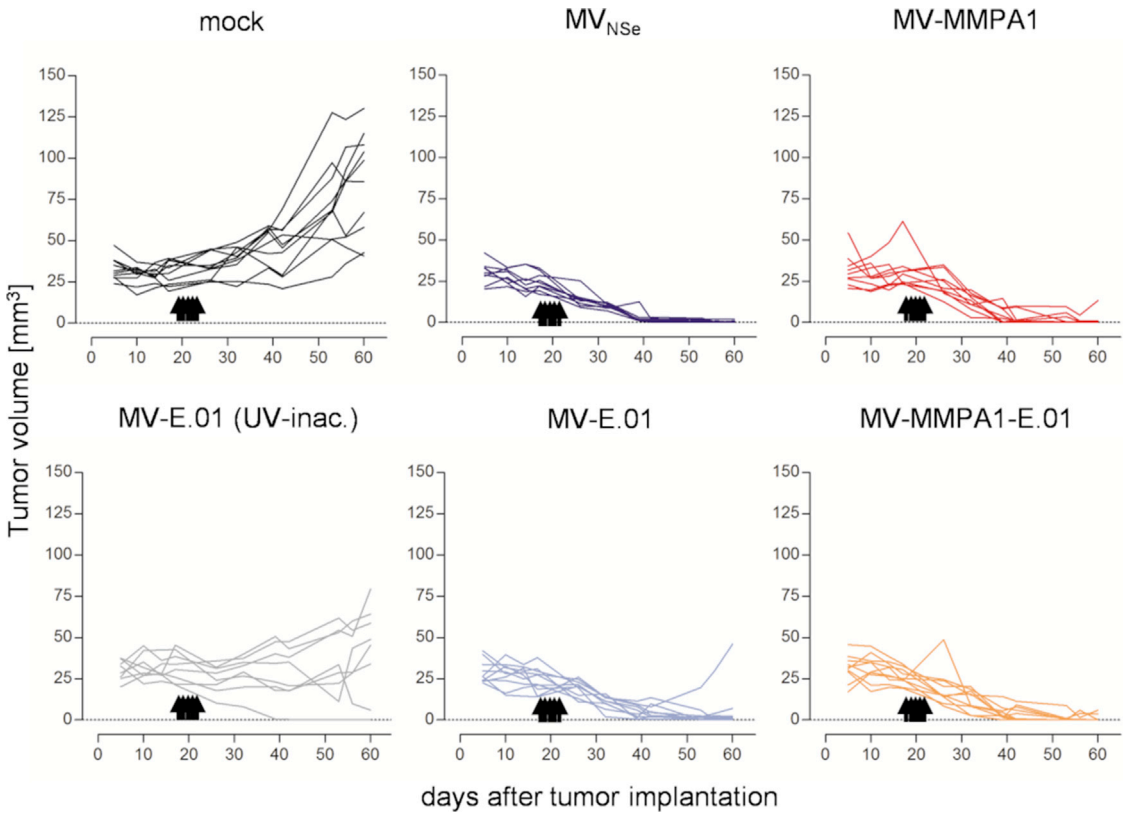

Figure 6. Efficacy of EGFR-, Protease-, or Dual-Targeted MeV *in vivo* in the LNZ-308 Model

Analysis of oncolytic efficacy in the EGFR/MMP double-positive, s.c. LNZ-308 tumor model in immunodeficient mice. Human xenograft tumor model in CD1-nude mice implanted subcutaneously with LNZ-308 cells in Matrigel. When first tumors started to grow, mice were injected i.t. on 5 consecutive days with indicated viruses or controls. n = 9–10. Tumor volume was monitored and growth of tumors is displayed. Each line represents tumor burden of one animal.

viruses seemed to be delayed and somewhat less efficient, since reduced maximal titers were observed. Interestingly, highest virus titers were observed at the moment of highest cell killing.

In addition, we validated cytotoxicity using the colony-forming assay. All cell lines were infected by all different viruses (MOI = 0.1) and survival of colony-forming entities was quantified (Figure 5B). For HT1080, all viruses cause a 10-fold reduction in CFUs. In LNZ-308 cultures, even a reduction by a factor of 100 was observed, i.e., 99% of colony-forming cells were eradicated by treatment of LNZ-308 cells by any of the tested viruses. Notably, only MV$_{NSe}$ and MV-E.01 were found to have a major impact on the number of colony-forming U87mg cells. Infection of U87mg cells by MV$_{NSe}$ reduced the number of colony-forming cells by a factor of more than 100. Strikingly, MV-E.01 reduced CFU numbers even approximately 1,000-fold, demonstrating enhanced cytolytic activity as compared to the non-targeted parental virus. Interestingly, MMP-targeted viruses reduced the number of CFU only about 2-fold when infecting U87mg cultures. However, in a low dilution of U87mg cells infected with either MMP-targeted virus, all cells were killed, most probably due to ongoing viral infection in these cultures, which had been diluted out in higher dilutions used for determination of CFU number (data not shown).

Oncolytic Activity of EGFR- and Dual-Targeted MeV *in vivo*

To test the anti-tumoral efficacy of EGFR- or dual-targeted MeV *in vivo*, we started with treatment of highly MeV-susceptible LNZ-308 tumors implanted into the flanks of CD1-nude mice. When tumor deposits had started to increase in volume between two different measurements in more than two thirds of the animals, all animals were treated by intratumoral (i.t.) injection with indicated viruses or control on 5 consecutive days (Figure 6). Mock-treated tumors revealed a 3-fold increase in tumor size over 40 days post treatment. In contrast, tumors of most animals treated by any oncolytic MeV shrunk and became not palpable, anymore, demonstrating significant oncolytic efficacy of all 4 tested viruses, irrespective of the targeting strategy (Figure 6). In the control group treated by inactivated virus, a slight delay of tumor growth became evident, while most animals still revealed steadily growing tumors. Because all inactivated virus batches demonstrated absence of residual infectivity before inoculation after incubating susceptible Vero-αHis-MMP14 cells with an aliquot of inactivate that would correspond to an MOI of 0.8 or 1.5

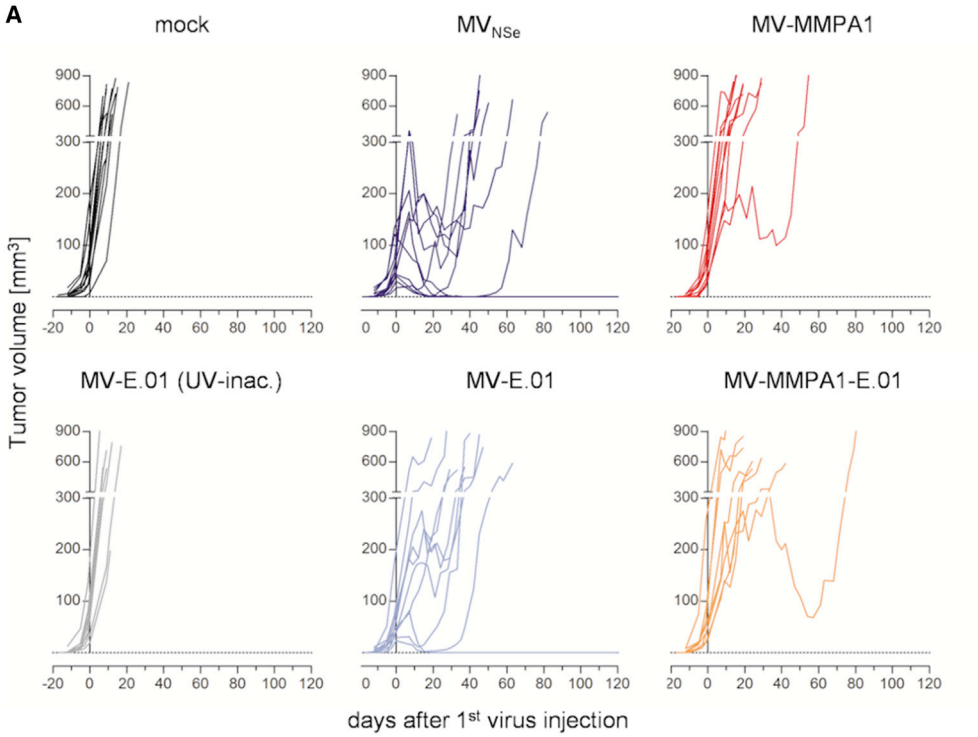

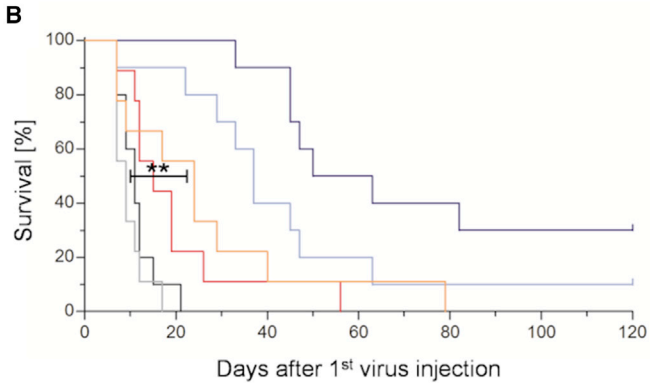

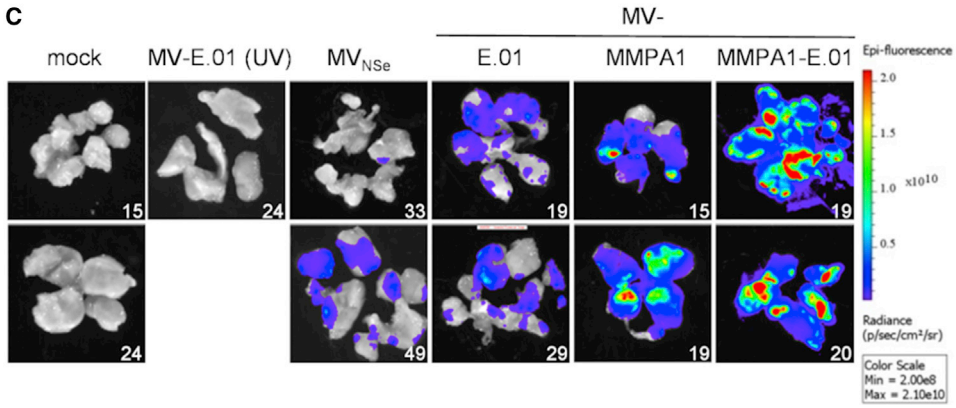

(legend on next page)

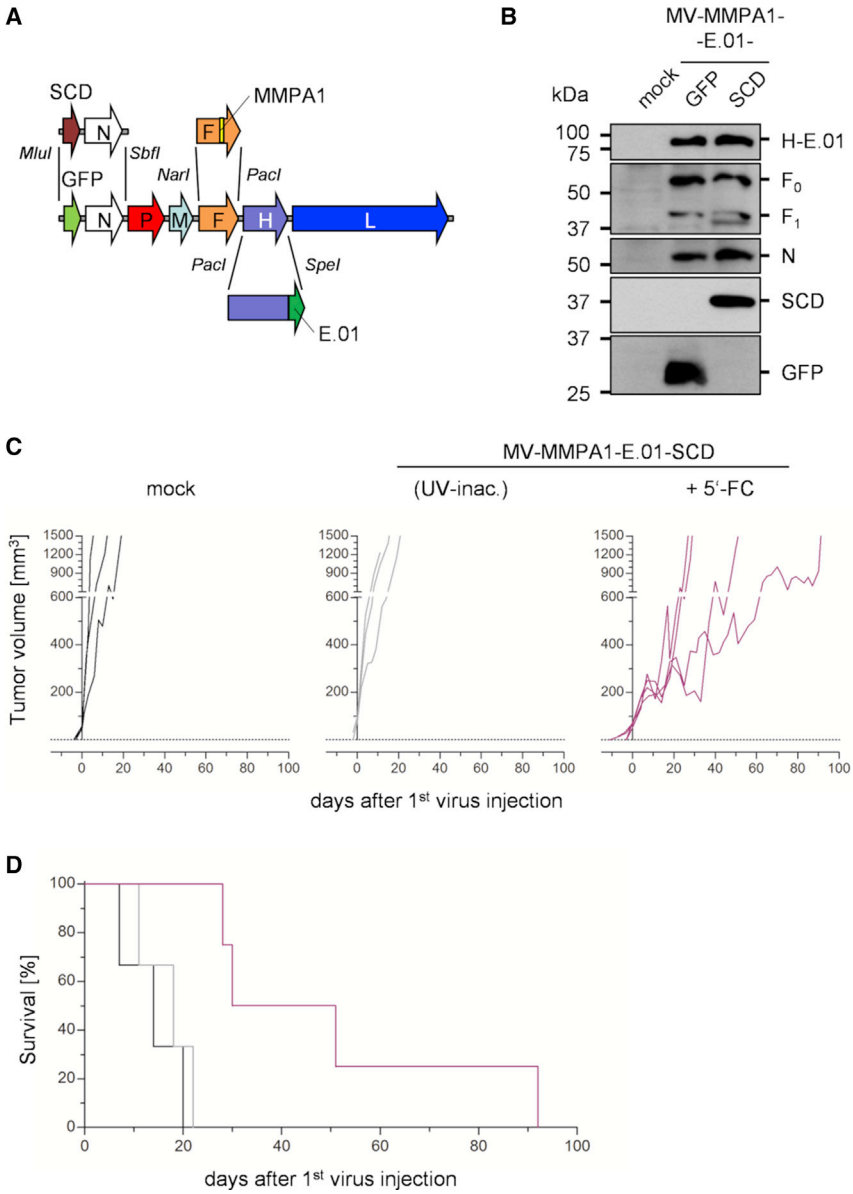

Figure 8. Generation and Efficacy of Armed Dual-Targeted Viruses

(A) Schematic representation of dual-targeted MeV genome with cloning sites used for exchange of the H and F gene cassette and the gene cassette encoding the prodrug convertase superCD in the first transcription unit. (B) Immunoblot for detection of marker protein or prodrug convertase encoding dual-targeted MeV. Lysates of infected HT1080 cells 48 h after infection (MOI = 0.1) were analyzed for indicated proteins. Protein content was normalized to MeV-N protein. (C and D) Analysis of oncolytic efficacy in the U87mg tumor model as presented in Figure 7, but animals were either treated with UV-inactivated or live MV-MMPA1-SCD(N)-E.01. The latter group was additionally treated with the prodrug 5-FC i.p. twice daily on 5 consecutive days in a dose of 200 μg/g body weight, when first tumors reached a volume of 800 mm^3. n = 3–4. (C) Tumor volume was monitored and growth of tumors is displayed. Each line represents tumor burden of one animal. (D) Survival of tumor-bearing animals. Kaplan-Meyer survival plots of treated animals.

before inactivation (data not shown), this effect cannot be linked to presence of residual active virus.

Switching to the *in vitro* less permissive U87mg tumors implanted in the flanks of SCID Cb17 mice, we observed exponential growth of tumors in mock-treated animals or animals treated with UV-inactivated, EGFR-targeted MV-E.01. Tumor growth was slowed down in all cohorts treated by active MeV (Figure 7A), which was reflected by significantly enhanced survival times of these animals (Figure 7B). In this animal model, protease targeting seems to impair direct oncolytic activity, reflected by faster tumor growth and lower median survival times, if compared to non-targeted or EGFR-targeted MeV. However, during preparation of tumors, when these had reached their maximal volume, we realized an unusual yellowish color of the tumor tissue especially in the groups treated by protease-targeted MeVs. When analyzing the tumors for GFP fluorescence, we observed high and wide-spread signals throughout these tumors presumably due to the presence of replicating, GFP-encoding MeV (Figure 7C). Highest signals were received from tumors of animals that had been treated by protease-targeted MeV, coinciding with the *in vitro* data using U87mg cells (Figure 5). This is indicating slower killing of U87mg cells by these viruses but still allowing spread of viruses. Therefore, we reasoned that virotherapeutic efficacy of the dual-targeted viruses

Figure 7. Efficacy and Spread of Targeted MeV *in vivo* in the U87mg Model

(A and B) Analysis of oncolytic efficacy in the EGFR/MMP double-positive, s.c. U87mg tumor model in immunodeficient mice. Human xenograft tumor model in SCID Cb17 mice implanted s.c. with U87mg cells. When tumors reached a volume of 30–50 mm^3, mice were injected i.t. on 5 consecutive days with indicated viruses or controls. n = 10–11. (A) Tumor volume was monitored and growth of tumors is displayed. Each line represents the tumor burden of one animal. (B) Survival of tumor-bearing animals. Kaplan-Meyer survival plots of treated animals. Log rank test, $^{**}p < 0.01$ (UV-inactivated versus MV-MMPA1-E.01). (C) Spread of oncolytic viruses throughout tumor tissue as evidenced by expression of the GFP marker protein. Tumors of individual mice were prepared and dissected at the indicated days post treatment. Subsequently, dissected tumors were imaged for GFP fluorescence using an IVIS Spectrum imaging system. Fluorescence intensities are displayed as indicated.

might be significantly enhanced also on less permissive tumors by arming these viruses with a prodrug convertase gene that takes advantage of the observed widespread distribution of the infection throughout the tumors.

Combination of Dual-Targeting with Arming of Oncolytic MeV

To generate such armed and dual-targeted viruses, the gene cassette encoding the marker GFP was exchanged against one encoding the prodrug convertase super cytosine deaminase (SCD) in the full-length genome allowing rescue of dual EGFR- and protease-targeted MeV (Figure 8A). The respective MV-MMPA1-E.01-SCD viruses (Table 1) were rescued and characterized by immunoblot for envelope protein modifications and expression of the additional gene cassette in direct comparison to the precursor virus MV-MMPA1-E.01 (Figure 8B). Indeed, envelope modifications targeting these viruses were conserved, while the marker protein expression was changed to expression of SCD. When applying this virus for treating subcutaneous (s.c.) U87mg tumors, tumor growth was delayed in the virus- and prodrug-treated animals (Figure 8C). Thereby, the virus- and prodrug-treated group reached a median survival of 50 days (Figure 8D) comparable to the survival of U87mg tumor-bearing mice treated with parental, non-targeted MV_{NSe} (Figure 7A and 7B). These data indicate that this combination is effective and could be higher compared to treatment by the dual- or protease-targeted MeV, alone, that had given rise to median survivals of about 25 days or 20 days post start of treatment, respectively, and even surpassed efficacy of EGFR-targeted MV-E.01 with a median survival of 40 days post treatment in the preceding experiments (Figures 7A and 7B).

DISCUSSION

In this study, we aimed to evaluate the therapeutic efficacy of EGFR-targeted oncolytic DARPin-MeV and the potential for combination of highly effective entry receptor targeting and protease targeting in one dual-targeted MeV to minimize off-target effects while preserving efficacy. We showed that EGFR-targeted MV-E.01 kills EGFR-positive tumor cells with comparable efficacy and kinetics than parental, non-targeted MV_{NSe} and also recognizes the glioblastoma-specific deletion-variant EGFRvIII as target receptor. Because we could also show that glioblastoma cell lines can be targeted via their protease profile, we next successfully generated dual-targeted MeV depending on the presence of both EGFR expression and protease activity of invasive tumors for spread and cell killing. Thereby, primary human keratinocytes, otherwise representing natural, EGFR-positive epithelial target cells of MeV, are spared from infection and related off-target effects. All these viruses proved to be effective *in vivo* in two different xenograft tumor models for GBM, albeit to a different extent in less protease-permissive U87mg tumors. However, the widespread infection of these tumors could be used for combination of prodrug convertase-armed, dual-targeted MeV with *in situ* chemotherapy.

These data provide evidence that EGFR-targeting using DARPins as targeting domains for oncolytic MeV works very efficiently. The kinetics of replication and cytotoxicity especially of MV-E.01 with the highest affinity DARPin was barely distinguishable from non-targeted parental MV_{NSe} on all 6 tested EGFR-positive tumor cell lines. Both other DARPins tested in this setting displayed graded efficacy correlating to their affinity for EGFR, thereby corroborating our analyses published before[12] on a broader basis of tested cell lines and with the kinetic component. As for scFvs,[30] affinity of the DARPin as targeting domain of re-targeted MeV is decisive for its efficacy. Moreover, EGFR-targeted MeV seemed even to kill tumor cells faster than MV_{NSe}. Also in combination with protease targeting, mice treated with dual-targeted MV-MMPA1-E.01 did even slightly better in the U87mg model than the MV-MMPA1 treated tumor-bearing animals. This is quite remarkable, because the density of EGFR on the tested cell lines is in the range of 5×10^3 to 4×10^4 molecules per cell[12], which is at least 10-fold lower than the density of the main targeted receptor, i.e., HER2/*neu*, in previous models tested for DARPin-MeV.[12,13]

While this dependence on the (natural) entry receptor density for efficient entry and spread of oncolytic MeV has been characterized to be a threshold correlation,[6] the threshold of EGFR for respectively targeted DARPin-MeV MV-E.01 would be quite low according to our data. The sufficiency of such low receptor levels can be explained by the high receptor affinity of this DARPin, as for an array of HER2/*neu*-targeted scFv-MeV oncolytic efficacy correlated with ligand affinity to the entry target receptor[30] and has also become apparent for HER2/*neu*-targeted or bivalent DARPin-MeV.[12,13] Indeed, the efficacy of the different EGFR-targeted DARPin-MeV tested here did correlate on all tested cell lines with the affinity of the used DARPin to EGFR both in cell killing and in reduction of CFUs in treated tumor cell cultures. In contrast, Sukksanpaisan et al. have described that in an ortho-topic xenograft model of ovarian carcinoma, receptor affinity of HER2/*neu*-targeted MeV did not correlate with therapeutic efficacy *in vivo*, but all viruses were comparably effective in terms of median survival of treated animals.[31] Interestingly, long-term surviving animals were nevertheless only found in high-affinity groups. If this holds true also for EGFR- or DARPin-targeting in general remains to be elucidated in future experiments.

Anyway, targeting of EGFR-positive tumors using DARPin E.01 rendered tumor marker-specific MeVs, which were at least as effective as non-targeted MeVs on most tumor cell lines *in vitro*, and of at least comparable efficacy in the LNZ-308 *in vivo* model. Also in combination with protease targeting, the dual-targeted MV-MMPA1-E.01 seemed to do even slightly better than solely protease-targeted MV-MMPA1. Therefore, both virus pairs indicate the excellent suitability and efficacy of (dual-)targeted DARPin-MeV using high-affinity DARPin E.01. Further demonstration of enhanced safety of the dual-targeted virus using *in vivo* models will be hard to establish due to the natural species specificity of MeV that would require at least triple genetic modification of the mouse strain to transgenically express both target receptors huCD46 and huEGFR in addition to a knockout of the murine interferon type-I system.[32,33] However, huEGFR knockin mice reveal signs of genotoxicity in the absence of any treatment[34], and it can be discussed, if toxicology studies in such modified mice with inherent phenotypes could be meaningful.

Toxicity of MeV infections is closely linked to the direct effects of MeV on infected host cells, e.g., immune cells.[35,36] The primary cytotoxic effect of MeV is the viral glycoprotein-mediated fusion of receptor-positive cells with infected neighboring cells. Thereby, giant multi-nucleated cells, so-called syncytia, are induced, which go into apoptosis within a few days.[6] Therefore, the prevention of this phenotype in primary human natural target cells of MeV infection, i.e., keratinocytes,[29] gives some confidence in a really meaningful readout for enhanced safety of the dual-targeted MV-MMPA1-E.01. Nevertheless, this virus still proved to be effective *in vivo* in a glioblastoma model, per se, while the attenuating effect of protease targeting can be utilized for the application of prodrug-convertase armed viruses. Intelligent combination of oncolytic MeV and (pro-)drug to trigger immunogenic cell death would be most desirable here and would therefore help to link direct oncolytic activity with immunotherapeutic mechanisms of virotherapy, as found for most successful oncolytic virus regimen that utilize induction of anti-tumoral immunity due to immunogenicity of OV-induced cell killing, which can be assisted by the expression of granulocyte-macrophage colony-stimulating factor (GM-CSF) *in situ* as an immune-modulatory cytokine. This setting that has gained market authorization of talimogene laherparepvec, an GM-CSF encoding oncolytic herpes simplex virus.[37]

Thus, the EGFR- or dual-targeted MeV generated here, which revealed their target specificity and efficacy *in vitro* and *in vivo*, provide further evidence for the versatility and efficacy of DARPin-targeting of oncolytic MeV (and most likely also of oncolytic vesicular stomatitis virus [VSV] pseudotyped by respectively modified MeV glycoproteins) for a relevant tumor entity with great medical need. Therefore, further development of these viruses appears quite promising to generate better armament to fight this devastating disease, especially with the potential for further arming these highly specific "magic bullets."

MATERIALS AND METHODS

Cells

Vero (African green monkey kidney; ATCC CCL-81), HT1080 (human fibrosarcoma; ATCC CLL-121), Huh7 (human hepatocellular carcinoma; Japanese Collection of Research Bioresources Cell Bank, Japan), SK-OV-3 (human ovarian carcinoma; ATCC HTB-77), CHO-K1 (ATCC CCL-61), and HEK293T (ATCC CRL-3216) cell lines were cultured in DMEM supplemented with 10% fetal bovine serum (FBS; Biochrom, Berlin, Germany) and 2 mM L-Gln (Biochrom). U87mg (human glioblastoma; ATCC HTB-14) and U87MG.ΔEGFR[38] cells were cultured in MEM (ThermoFisher Scientific, Ulm, Germany) with 10% FBS, 2 mM L-Gln, 1 mM sodium pyruvate, 3.35 g/L $NaHCO_3$, and 1% non-essential amino acids. Vero-αHis[10], LNT-229, and LNZ-308 cells[39] and their maintenance have been described. CHO-EGFR clone 22.2 cells have been described[12] and were cultured in DMEM + 10% FBS, 2 mM L-Gln, and 0.5 mg/mL G418 (GIBCO-BRL, Eggenstein, Germany). Human primary keratinocytes were cultured in serum-free keratinocyte growth medium (Provitro, Berlin, Germany).

293T-F cells stably expressing F were generated by transfection of pCG-F-IRES-Puro into HEK293T cells using Lipofectamine 2000 (ThermoFisher Scientific) according to the manufacturer's instruction. Transfected cells were selected using 1 μg/mL Puromycin starting 48 h after transfection. F expression of single cell clones was analyzed by western blot analysis or flow cytometry. Vero-αHis-MMP14 cells were generated by transduction with a VSV-G pseudotyped, HIV-1-based lentiviral vector system[40] using pH-MMP14-IN (kind gift of I. Schneider) as transfer vector. Cells were cultivated for 2 weeks with 0.5 mg/mL G418 to select transduced cells. Thereafter, single cell clones were generated by limiting dilution and their suitability for MMP-activatable MeV infection was tested by infection of respective clones by MV-MMPA1. To select the best MeV-producing clone, we compared all MV-MMPA1-susceptible clones (formation of syncytia) by analyzing viral titers produced using the respective clones for virus amplification.

The CHO-EGFRvIII cell line stably expressing EGFRvIII was generated by lipofection of pcDNA3.1(+)-EGFRvIII into CHO-K1 cells and selection of stably transfected clones using 1.2 mg/mL G418 (GIBCO-BRL). Single cell clones generated via limiting dilution were analyzed for EGFRvIII expression by flow cytometry. For limiting dilution, G418-selected cells were seeded in 96 well plates with a cell count of 0.3 cells per well. Growing colonies were expanded after 1 to 2 weeks and analyzed for homogeneous transgene expression by flow cytometry. All cells were cultured at 37°C in a humidified atmosphere containing 6% CO_2 for a maximum of 6 months of culture after thawing of the original stock.

Plasmids

The plasmid p(+)PolII-MV_{NSe}-MMPA1-GFP(N)-E.01, encoding the genome of the dual-targeted virus, was cloned using the plasmid p(+)PolII-MV_{NSe}-MMPA1-GFP(N), encoding the genome of the MMP-targeted virus,[27] and exchanging the H cassette via *PacI*/*SpeI* (NEB, Frankfurt, Germany). By exchanging the *gfp* marker gene against the prodrug convertase SCD encoding *scd* gene via the DNA fragment also containing the MeV N gene cassette by *Mlu*I/*SbfI* (NEB), plasmid p(+)PolII-MV_{NSe}-MMPA1-SCD(N)-E.01 was generated. The expression plasmid pCG-F-IRES-Puro allowing selection of MeV-F expression by coupling F mRNA to puromycin resistance was generated by blunt end insertion of the IRES-Puromycin cassette released from pH-HCD30-IP-LTR[41] via *Spe*I and *Acc65*I 3′ to the F gene by linearization of pCG-F[42] using *XbaI* (NEB) and subsequent *Klenow* (NEB) digestion to generate blunt ends and allowing ligation. EGFRvIII sequence was obtained by RNA isolation from U87MG.ΔEGFR cells that express EGFRvIII as a transgene. Isolated mRNA was used for subsequent cDNA synthesis with oligo dT primers (ThermoFisher Scientific) and PCR with ORF-flanking primers additionally encompassing HindIII (5′) (5′-AAGCTTATGCGACCCTCCGGAACGGC CGG-3′) and *XbaI* (3′) (5′-TCTAGATCATGCTCCAATAAATT CACTGC-3′) restriction sites. The PCR product was directly cloned by TOPO TA cloning into pCR2.1-Topo (ThermoFisher Scientific), and the correct nucleotide sequence of the cloned amplicon was confirmed by sequencing the full ORF (Eurofins Scientific, Hamburg,

Germany). The gene encoding EGFRvIII was finally inserted using *Hind*III/*Xba*I restriction into the MCS of the G418-selectable expression plasmid pcDNA3.1(+) (ThermoFisher Scientific) to yield pcDNA3.1(+)-EGFRvIII.

Viruses

MV_{NSe}-GFP(N) (MV_{Nse}), MV_{NSe}-GFP(N)-E.01 (MV-E.01), MV_{NSe}-GFP(N)-E.68 (MV-E.68), and MV_{NSe}-GFP(N)-E.69 (MV-E.69) were previously generated,[12] as well as MMP-targeted MV_{NSe}-MMPA1-GFP(N) (MV-MMPA1).[26] Dual-targeted MV_{NSe}-MMPA1-GFP(N)-E.01 (MV-MMPA1-E.01) and prodrug convertase-armed, dual-targeted MV_{NSe}-MMPA1-SCD(N)-E.01 (MV-MMPA1-E.01-SCD) were generated using the full genome-encoding plasmids p(+)PolII-MVNSe-MMPA1-GFP(N)-E.01 and p(+)PolII-MVNSe-MMPA1-SCD(N)-E.01, respectively, utilizing the PolII-rescue system,[43] as described, but using 293T-F cells for transfection, which were overlaid onto sub-confluent MMP-positive HT1080 cells for amplification. Overlay cultures were closely monitored for isolated syncytia, which indicated monoclonal replicative centers. Single syncytia were picked and overlaid onto 50% confluent cells cultured in 6-well plates and harvested as passage 0 (P0) by scraping and a freeze-thaw cycle of cells at the time of maximal infection. Subsequent passages were generated after titration to determine the 50% $TCID_{50}$ of infectious virus according to the method of Kaerber and Spaerman[44] and infection of cells at a MOI of 0.03. The viruses were passaged up to 5 passages at the maximum. MV_{NSe} was amplified on Vero cells, EGFR-targeted MV-E.01 was amplified on Vero-αHis cells, while all protease-targeted viruses were amplified on EGFR- and MMP-positive HT1080 cells or Vero-αHis-MMP14 cells. All virus stocks were stored in aliquots at −80°C.

Virus Growth Kinetics

Cells were seeded in 12-well plates (Nunc Delta Surface; Nunc, Wiesbaden, Germany). Cells were infected at an MOI of 0.03 in a total of 1 mL medium. At the indicated time points, supernatants were clarified by centrifugation and stored in aliquots at −80°C. Infected cells were scraped into 1 mL OptiMEM and subjected to a freeze-thaw cycle. After thawing, supernatants containing released particles were also clarified by centrifugation and stored in aliquots at −80°C. Cell-associated virus titers and titers of virus in supernatants were determined by $TCID_{50}$ titration. Viral titers were analyzed 48 h after infection.

Immunoblotting

HT1080 cells were infected with recombinant MeV at an MOI of 0.1 and cells were lysed 48 h p.i. using RIPA lysis-buffer (50 mM Tris, 150 mM NaCl, 1% NP-40 [w/v], 0.5% Na-desoxycholate [w/v], 0.1% SDS [w/v], pH 8.0) supplemented with Protease Inhibitor Cocktail Complete (Roche Diagnostics, Mannheim, Germany). The cell lysates were mixed 1:1 with 2× urea sample buffer (200 mM Tris-HCl [pH 6.8], 8 M urea, 5% SDS [w/v], 0.1 mM EDTA, 0.03% bromphenol blue [w/v], 1.5% dithiothreitol [w/v]), and denatured for 10 min at 95°C, then fractionated by SDS-PAGE, and blotted onto PVDF membranes (Hybond-P, GE Healthcare, München, Germany). Membranes were blocked with 5% milk powder in TBS plus 0.1% Tween for 1 h at room temperature. Rabbit anti-H_{cyt} serum (Eurogentec, Seraing, Belgium; 1:20,000), rabbit anti-F cytoplasmic tail serum (anti-F_{cyt};[45] 1:10,000), rabbit anti-N (ab23974; Abcam, Cambridge, UK; 1:25,000), or mouse anti-β-actin (ab6276 [AC-15]; Abcam; 1:5,000), rabbit anti-GFP (A-11122; ThermoFisher Scientific; 1:2,000), or sheep anti-yeast CD (2485-4906; Bio-Rad AbD Serotec, Puchheim, Germany; 1:500) were used as primary antibody for MeV-H, MeV-N, β-actin, GFP, or SuperCD detection, respectively. A donkey HRP-coupled anti-rabbit immunoglobulin G (IgG) (H&L) polyclonal antibody (611-7302; Rockland, Gilbertsville, PA, 1:10,000), anti-mouse IgG+A+M (646420; ThermoFisher Scientific; 1:10,000), or anti-sheep IgG (whole molecule) (A3415; Sigma-Aldrich; 1:5,000) served as secondary antibodies, as appropriate. Peroxidase activity was visualized with the ECL Plus Western Blotting Detection System (GE Healthcare) on Amersham Hyperfilm ECL (GE Healthcare).

Flow Cytometry Analysis

Flow cytometry was performed on an LSRII-SORP FACS (BD, Heidelberg, Germany) and data were analyzed using the FACSDiva version 6.1.3 or FCS Express version 3. Cells were stained and analyzed as described before[40] using the following antibodies: mouse anti-hu EGFR-PE (clone 582; Santa Cruz, Heidelberg, Germany), mouse anti-hu EGFRvIII (L8A4),[46] or mouse anti-MV-F (F_{Y503})[47] in combination with goat anti-mouse IgG-PE (550589, BD; 1:50).

Infection Assays

Respective cells were seeded in 6-well tissue culture plates (Nunc), infected with recombinant MeV at an MOI of 0.1, 0.3, or 1.0, and subsequently cultured at 37°C. Syncytia formation was analyze 48 to 72 h after infection by fluorescence microscopy (Axiovert 25 or 200M; Zeiss, Göttingen, Germany). The MMP inhibitor GM6001 (Calbiochem, Merck KGaA, Darmstadt, Germany) was supplemented in indicated experiments after transfection to a final concentration of 10 mM.

In vitro Cytotoxicity

Respective cells of interest (1×10^4) were seeded into 96-well plates (Nunc) and infected with recombinant MeV (MOI = 1) or left uninfected (mock) 4 h after seeding in quadruplicates. Viability of the cells after infection was determined using MTT (Cell Proliferation Kit I; Roche Diagnostics). Cells were incubated with the MTT solution for 4 h and then solubilization solution was added 72 h after infection. Following overnight incubation, a formazan dye was formed, which was quantified in quadruplicates using an ELISA reader (Multiskan RC; Thermo Labsystems, Dreieich, Germany). Averages of the replicates were calculated and values of virus infected samples were divided by those of uninfected controls to calculate relative cytotoxicity in %.

Colony-Forming Assay

Tumor cells were infected 4 h after seeding of 5×10^5 cells in a 6-well plate in triplicates with recombinant MeV (MOI = 0.1) or left untreated. 72 h after infection, the surviving cells were trypsinized,

serially diluted, replated in 6-well plates, and incubated for 2 to 3 weeks to allow colony formation (50–100 cells/colony). Cells were then fixed with 10% PFA (w/v) for 4 h and subsequently stained with crystal violet solution (PBS, 18% ethanol [v/v], 0.1% crystal violet [w/v]). Only colonies that were well separated from each other and contained >50 cells were counted.

Animal Experiments

Experimental mouse work was carried out in compliance with the regulations of the German animal protection law and as authorized by the RP Darmstadt. To evaluate the oncolytic efficacy *in vivo*, we s.c. injected 1×10^7 LNZ-308 or 2×10^6 U87mg cells in 100 µL 50% Matrigel (ThermoFisher Scientific) solution or PBS, respectively, into the flanks of 6- to 8-week-old CD1-nude or SCID Cb-17 mice (Charles River, Köln, Germany), respectively. When LNZ-308 tumors started to grow or U87mg tumors reached a size of 50–100 mm^3, mice were randomized into groups. They received i.t. injections with a dose of 1×10^6 $TCID_{50}$/injection MeV in 100 µL OptiMEM (ThermoFisher Scientific) on 5 consecutive days. Control animals were injected with 100 µL OptiMEM (mock), or with 100 µL UV-inactivated virus (120,000 µJ/cm^2 UV light [254 nm], 90 min). For tumors treated with active MV-MMPA1-SCD(N)-E.01, 5-fluorocytosine was applied i.p. twice daily on 5 consecutive days in a dose of 200 µg/g body weight when the first tumors reached a volume of 800 mm^3. Tumor volumes were determined twice a week. Animals were euthanized, when the tumor volume reached 1,500 mm^3, mice lost more than 20% of body weight, or tumor ulceration occurred.

AUTHOR CONTRIBUTIONS

M.D.M. was responsible for the design of the entire study. U.M.L. and J.R.H.H. contributed important aspects for the design and conduction of the studies. J.R.H.H. and V.K. conducted all experiments. Data analysis was performed by J.R.H.H., V.K., and M.D.M. J.R.H.H. and M.D.M. wrote the first draft of the manuscript and designed figures. All authors edited and approved the final version of the manuscript.

CONFLICTS OF INTEREST

U.M.L. holds patents describing the combination of the super-cytosine deaminase prodrug convertase gene with Schwarz strain-derived oncolytic MeV.

ACKNOWLEDGMENTS

We thank Urs Schneider for providing the PolII Rescue System for measles viruses, Stephen J. Russell for Vero-αHis, Frank Furnari and Webster Cavenee for U87MG.ΔEGFR, and Monika E. Hegi for LNT-229 and LNZ-308 cells via Ulrike Naumann. The authors are grateful to Andreas Plückthun for providing DARPins E.01, E.68, and E.69, to Roberto Cattaneo for providing F_{Y503} anti-MeV-F antibody, to D.D. Bigner for providing L8A4 anti-huEGFRvIII antibody, and Irene Schneider for providing the plasmid pH-MMP14-IN. We are indebted to Steffen Prüfer, Larissa Angebauer, Matthias Dusemund, Jürgen Schnotz, and Dorothea Kreuz for excellent technical assistance and Roland Plesker for assistance in animal experiments. This work was performed in Langen, Germany. M.D.M. received funding from the Deutsche Krebshilfe (109614).

REFERENCES

1. Tatsuo, H., Ono, N., Tanaka, K., and Yanagi, Y. (2000). SLAM (CDw150) is a cellular receptor for measles virus. Nature *406*, 893–897.
2. Mühlebach, M.D., Mateo, M., Sinn, P.L., Prüfer, S., Uhlig, K.M., Leonard, V.H., Navaratnarajah, C.K., Frenzke, M., Wong, X.X., Sawatsky, B., et al. (2011). Adherens junction protein nectin-4 is the epithelial receptor for measles virus. Nature *480*, 530–533.
3. Noyce, R.S., Bondre, D.G., Ha, M.N., Lin, L.T., Sisson, G., Tsao, M.S., and Richardson, C.D. (2011). Tumor cell marker PVRL4 (nectin 4) is an epithelial cell receptor for measles virus. PLoS Pathog. *7*, e1002240.
4. Dörig, R.E., Marcil, A., Chopra, A., and Richardson, C.D. (1993). The human CD46 molecule is a receptor for measles virus (Edmonston strain). Cell *75*, 295–305.
5. Naniche, D., Varior-Krishnan, G., Cervoni, F., Wild, T.F., Rossi, B., Rabourdin-Combe, C., and Gerlier, D. (1993). Human membrane cofactor protein (CD46) acts as a cellular receptor for measles virus. J. Virol. *67*, 6025–6032.
6. Anderson, B.D., Nakamura, T., Russell, S.J., and Peng, K.-W. (2004). High CD46 receptor density determines preferential killing of tumor cells by oncolytic measles virus. Cancer Res. *64*, 4919–4926.
7. Msaouel, P., Opyrchal, M., Dispenzieri, A., Peng, K.W., Federspiel, M.J., Russell, S.J., and Galanis, E. (2018). Clinical Trials with Oncolytic Measles Virus: Current Status and Future Prospects. Curr. Cancer Drug Targets *18*, 177–187.
8. Russell, S.J., Federspiel, M.J., Peng, K.W., Tong, C., Dingli, D., Morice, W.G., Lowe, V., O'Connor, M.K., Kyle, R.A., Leung, N., et al. (2014). Remission of disseminated cancer after systemic oncolytic virotherapy. Mayo Clin. Proc. *89*, 926–933.
9. Vongpunsawad, S., Oezgun, N., Braun, W., and Cattaneo, R. (2004). Selectively receptor-blind measles viruses: Identification of residues necessary for SLAM- or CD46-induced fusion and their localization on a new hemagglutinin structural model. J. Virol. *78*, 302–313.
10. Nakamura, T., Peng, K.W., Vongpunsawad, S., Harvey, M., Mizuguchi, H., Hayakawa, T., Cattaneo, R., and Russell, S.J. (2004). Antibody-targeted cell fusion. Nat. Biotechnol. *22*, 331–336.
11. Nakamura, T., Peng, K.W., Harvey, M., Greiner, S., Lorimer, I.A., James, C.D., and Russell, S.J. (2005). Rescue and propagation of fully retargeted oncolytic measles viruses. Nat. Biotechnol. *23*, 209–214.
12. Friedrich, K., Hanauer, J.R., Prüfer, S., Münch, R.C., Völker, I., Filippis, C., Jost, C., Hanschmann, K.M., Cattaneo, R., Peng, K.W., et al. (2013). DARPin-targeting of measles virus. Unique bispecificity, effective oncolysis, and enhanced safety. Mol. Ther. *21*, 849–859.
13. Hanauer, J.R., Gottschlich, L., Riehl, D., Rusch, T., Koch, V., Friedrich, K., Hutzler, S., Prüfer, S., Friedel, T., Hanschmann, K.M., et al. (2016). Enhanced lysis by bispecific oncolytic measles viruses simultaneously using HER2/neu or EpCAM as target receptors. Mol. Ther. Oncolytics *3*, 16003.
14. Allen, C., Vongpunsawad, S., Nakamura, T., James, C.D., Schroeder, M., Cattaneo, R., Giannini, C., Krempski, J., Peng, K.W., Goble, J.M., et al. (2006). Retargeted oncolytic measles strains entering via the EGFRvIII receptor maintain significant antitumor activity against gliomas with increased tumor specificity. Cancer Res. *66*, 11840–11850.
15. Paraskevakou, G., Allen, C., Nakamura, T., Zollman, P., James, C.D., Peng, K.W., Schroeder, M., Russell, S.J., and Galanis, E. (2007). Epidermal growth factor receptor (EGFR)-retargeted measles virus strains effectively target EGFR- or EGFRvIII expressing gliomas. Mol. Ther. *15*, 677–686.
16. Karsy, M., Gelbman, M., Shah, P., Balumbu, O., Moy, F., and Arslan, E. (2012). Established and emerging variants of glioblastoma multiforme: review of morphological and molecular features. Folia Neuropathol. *50*, 301–321.
17. Mehta, M., Wen, P., Nishikawa, R., Reardon, D., and Peters, K. (2017). Critical review of the addition of tumor treating fields (TTFields) to the existing standard of care for newly diagnosed glioblastoma patients. Crit. Rev. Oncol. Hematol. *111*, 60–65.
18. Platten, M. (2019). How to integrate immunotherapy into standard of care in glioblastoma. Neuro-oncol. *21*, 699–700.

19. Libermann, T.A., Nusbaum, H.R., Razon, N., Kris, R., Lax, I., Soreq, H., Whittle, N., Waterfield, M.D., Ullrich, A., and Schlessinger, J. (1985). Amplification, enhanced expression and possible rearrangement of EGF receptor gene in primary human brain tumours of glial origin. Nature *313*, 144–147.

20. Frederick, L., Eley, G., Wang, X.Y., and James, C.D. (2000). Analysis of genomic rearrangements associated with EGRFvIII expression suggests involvement of Alu repeat elements. Neuro-oncol. *2*, 159–163.

21. Vogel, A., Hofheinz, R.D., Kubicka, S., and Arnold, D. (2017). Treatment decisions in metastatic colorectal cancer - Beyond first and second line combination therapies. Cancer Treat. Rev. *59*, 54–60.

22. Steiner, D., Forrer, P., and Plückthun, A. (2008). Efficient selection of DARPins with sub-nanomolar affinities using SRP phage display. J. Mol. Biol. *382*, 1211–1227.

23. Ensslin, C.J., Rosen, A.C., Wu, S., and Lacouture, M.E. (2013). Pruritus in patients treated with targeted cancer therapies: systematic review and meta-analysis. J. Am. Acad. Dermatol. *69*, 708–720.

24. Ocvirk, J., Heeger, S., McCloud, P., and Hofheinz, R.-D. (2013). A review of the treatment options for skin rash induced by EGFR-targeted therapies: Evidence from randomized clinical trials and a meta-analysis. Radiol. Oncol. *47*, 166–175.

25. Rosen, A.C., Case, E.C., Dusza, S.W., Balagula, Y., Gordon, J., West, D.P., and Lacouture, M.E. (2013). Impact of dermatologic adverse events on quality of life in 283 cancer patients: a questionnaire study in a dermatology referral clinic. Am. J. Clin. Dermatol. *14*, 327–333.

26. Springfeld, C., von Messling, V., Frenzke, M., Ungerechts, G., Buchholz, C.J., and Cattaneo, R. (2006). Oncolytic efficacy and enhanced safety of measles virus activated by tumor-secreted matrix metalloproteinases. Cancer Res. *66*, 7694–7700.

27. Mühlebach, M.D., Schaser, T., Zimmermann, M., Armeanu, S., Hanschmann, K.M., Cattaneo, R., Bitzer, M., Lauer, U.M., Cichutek, K., and Buchholz, C.J. (2010). Liver cancer protease activity profiles support therapeutic options with matrix metalloproteinase-activatable oncolytic measles virus. Cancer Res. *70*, 7620–7629.

28. Kast, R.E., and Halatsch, M.-E. (2012). Matrix metalloproteinase-2 and -9 in glioblastoma: a trio of old drugs-captopril, disulfiram and nelfinavir-are inhibitors with potential as adjunctive treatments in glioblastoma. Arch. Med. Res. *43*, 243–247.

29. Gourru-Lesimple, G., Mathieu, C., Thevenet, T., Guillaume-Vasselin, V., Jégou, J.F., Boer, C.G., Tomczak, K., Bloyet, L.M., Giraud, C., Grande, S., et al. (2017). Measles virus infection of human keratinocytes: Possible link between measles and atopic dermatitis. J. Dermatol. Sci. *86*, 97–105.

30. Hasegawa, K., Hu, C., Nakamura, T., Marks, J.D., Russell, S.J., and Peng, K.W. (2007). Affinity thresholds for membrane fusion triggering by viral glycoproteins. J. Virol. *81*, 13149–13157.

31. Suksanpaisan, L., Russell, S.J., and Peng, K.-W. (2014). High scFv-receptor affinity does not enhance the antitumor activity of HER2-retargeted measles virus. Cancer Gene Ther. *21*, 256–260.

32. Mrkic, B., Pavlovic, J., Rülicke, T., Volpe, P., Buchholz, C.J., Hourcade, D., Atkinson, J.P., Aguzzi, A., and Cattaneo, R. (1998). Measles virus spread and pathogenesis in genetically modified mice. J. Virol. *72*, 7420–7427.

33. Mura, M., Ruffié, C., Combredet, C., Aliprandini, E., Formaglio, P., Chitnis, C.E., Amino, R., and Tangy, F. (2019). Recombinant measles vaccine expressing malaria antigens induces long-term memory and protection in mice. npj Vaccines *4*, 12.

34. Sibilia, M., Wagner, B., Hoebertz, A., Elliott, C., Marino, S., Jochum, W., and Wagner, E.F. (2003). Mice humanised for the EGF receptor display hypomorphic phenotypes in skin, bone and heart. Development *130*, 4515–4525.

35. Laksono, B.M., de Vries, R.D., Verburgh, R.J., Visser, E.G., de Jong, A., Fraaij, P.L.A., Ruijs, W.L.M., Nieuwenhuijse, D.F., van den Ham, H.J., Koopmans, M.P.G., et al. (2018). Studies into the mechanism of measles-associated immune suppression during a measles outbreak in the Netherlands. Nat. Commun. *9*, 4944.

36. Laksono, B.M., Grosserichter-Wagener, C., de Vries, R.D., Langeveld, S.A.G., Brem, M.D., van Dongen, J.J.M., Katsikis, P.D., Koopmans, M.P.G., van Zelm, M.C., and de Swart, R.L. (2018). In Vitro Measles Virus Infection of Human Lymphocyte Subsets Demonstrates High Susceptibility and Permissiveness of both Naive and Memory B Cells. J. Virol. *92*, e00131–18.

37. Andtbacka, R.H.I., Kaufman, H.L., Collichio, F., Amatruda, T., Senzer, N., Chesney, J., Delman, K.A., Spitler, L.E., Puzanov, I., Agarwala, S.S., et al. (2015). Talimogene Laherparepvec Improves Durable Response Rate in Patients With Advanced Melanoma. J. Clin. Oncol. *33*, 2780–2788.

38. Nishikawa, R., Ji, X.D., Harmon, R.C., Lazar, C.S., Gill, G.N., Cavenee, W.K., and Huang, H.J. (1994). A mutant epidermal growth factor receptor common in human glioma confers enhanced tumorigenicity. Proc. Natl. Acad. Sci. USA *91*, 7727–7731.

39. Albertoni, M., Shaw, P.H., Nozaki, M., Godard, S., Tenan, M., Hamou, M.F., Fairlie, D.W., Breit, S.N., Paralkar, V.M., de Tribolet, N., et al. (2002). Anoxia induces macrophage inhibitory cytokine-1 (MIC-1) in glioblastoma cells independently of p53 and HIF-1. Oncogene *21*, 4212–4219.

40. Funke, S., Maisner, A., Mühlebach, M.D., Koehl, U., Grez, M., Cattaneo, R., Cichutek, K., and Buchholz, C.J. (2008). Targeted cell entry of lentiviral vectors. Mol. Ther. *16*, 1427–1436.

41. Hanauer, J.D.S., Rengstl, B., Kleinlützum, D., Reul, J., Pfeiffer, A., Friedel, T., Schneider, I.C., Newrzela, S., Hansmann, M.L., Buchholz, C.J., and Muik, A. (2018). CD30-targeted oncolytic viruses as novel therapeutic approach against classical Hodgkin lymphoma. Oncotarget *9*, 12971–12981.

42. Cathomen, T., Buchholz, C.J., Spielhofer, P., and Cattaneo, R. (1995). Preferential initiation at the second AUG of the measles virus F mRNA: a role for the long untranslated region. Virology *214*, 628–632.

43. Martin, A., Staeheli, P., and Schneider, U. (2006). RNA polymerase II-controlled expression of antigenomic RNA enhances the rescue efficacies of two different members of the Mononegavirales independently of the site of viral genome replication. J. Virol. *80*, 5708–5715.

44. Kärber, G. (1931). Beitrag zur kollektiven Behandlung pharmakologischer Reihenversuche. *Archiv f. experiment. Pathol. u.* Pharmakol *162*, 480–483.

45. Cattaneo, R., and Rose, J.K. (1993). Cell fusion by the envelope glycoproteins of persistent measles viruses which caused lethal human brain disease. J. Virol. *67*, 1493–1502.

46. Wikstrand, C.J., Hale, L.P., Batra, S.K., Hill, M.L., Humphrey, P.A., Kurpad, S.N., McLendon, R.E., Moscatello, D., Pegram, C.N., Reist, C.J., et al. (1995). Monoclonal antibodies against EGFRvIII are tumor specific and react with breast and lung carcinomas and malignant gliomas. Cancer Res. *55*, 3140–3148.

47. Vincent, S., Spehner, D., Manié, S., Delorme, R., Drillien, R., and Gerlier, D. (1999). Inefficient measles virus budding in murine L.CD46 fibroblasts. Virology *265*, 185–195.